The influence of secretory-protein charge on late stages of secretion from the Gram-positive bacterium *Bacillus subtilis*

Keith STEPHENSON*[1], Christina L. JENSEN‡[2], Steen T. JØRGENSEN‡, Jeremy H. LAKEY† and Colin R. HARWOOD*[3]

*Department of Microbiology and Immunology, The Medical School, University of Newcastle upon Tyne, Framlington Place, Newcastle upon Tyne, NE2 4HH, U.K., †School of Biochemistry and Genetics, The Medical School, University of Newcastle upon Tyne, Framlington Place, Newcastle upon Tyne, NE2 4HH, U.K., and ‡Bacterial Gene Technology, Novo Nordisk A/S, DK-2880 Bagsværd, Denmark

Following their secretion across the cytoplasmic membrane, processed secretory proteins of *Bacillus subtilis* must fold into their native conformation prior to translocation through the cell wall and release into the culture medium. The rate and efficiency of folding are critical in determining the yields of intact secretory proteins. The *B. subtilis* membrane is surrounded by a thick cell wall comprising a heteropolymeric matrix of peptidoglycan and anionic polymers. The latter confer a high density of negative charge on the wall, endowing it with ion-exchange properties, and secretory proteins destined for the culture medium must traverse the wall as the last stage in the export process. To determine the influence of charge on late stages in the secretion of proteins from this bacterium, we have used sequence data from two related α-amylases, to engineer the net charge of AmyL, an α-amylase from *Bacillus licheniformis* that is normally secreted efficiently from *B. subtilis*. While AmyL has a pI of 7.0, chimaeric enzymes with pI values of 5.0 and 10.0 were produced and characterized. Despite the engineered changes to their physico-chemical properties, the chimaeric enzymes retained many of the enzymic characteristics of AmyL. We show that the positively charged protein interacts with the cell wall in a manner that influences its secretion.

Key words: protein secretion, protein engineering, cell walls, α-amylase.

INTRODUCTION

Members of the genus *Bacillus* have the capacity to secrete proteins directly into the culture medium at concentrations in excess of 5 g/litre [1]. Following translation, pre-secretory proteins are targeted to the membrane, where they are actively translocated to the *trans* side of the cytoplasmic membrane via the integral membrane pre-secretory protein translocase, concomitant with the removal of the N-terminal signal peptide by membrane-inserted signal peptidases [2].

On the *trans* side of the membrane, mature secretory proteins fold into their native conformations in a process that is rate limiting for secretion and which is accompanied by the release of the protein from the membrane [3]. The rate and efficiency of this folding step are critical in determining the final yields of intact secretory proteins which are released into the culture medium of *Bacillus subtilis*, since slowly folding proteins can undergo extensive degradation prior to attaining the fully folded and, usually, protease-resistant, conformation [4].

Following the removal of the signal peptide, but before release into the culture medium, certain secretory proteins are subjected to considerable cell-associated degradation in *B. subtilis* [5]. We have recently shown that a cell-wall-binding protein (CWBP)52, a serine protease, is involved in the cell-associated degradation of a *B. licheniformis* α-amylase (AmyL) when secreted from *B. subtilis* [6]. It is likely that proteases at the membrane/wall interface perform a clearing function by removing slowly folding or misfolded proteins from the vicinity of the translocase, thereby avoiding potentially lethal blockages of the secretion pathway and ensuring the fidelity of the secretion process [7,8].

The cell envelope of *B. subtilis* consists of a single (cytoplasmic) membrane surrounded by a thick cell wall which is composed of a heteropolymeric matrix of peptidoglycan [9] and covalently attached anionic polymers [10]. The anionic polymers teichoic or teichuronic acid, which can account for up to 50 % of the weight of the wall, confer a high degree of negative charge to the wall and contribute to the specific surface-charge properties of the cell [11]. In addition to wall teichoic acids, *B. subtilis* also has membrane-anchored lipoteichoic acids [12,13].

The high density of negative charge provided by the phosphate or carboxy groups of anionic polymers endows the cell wall with ion-exchange properties, within which charged entities, such as proteins or cations, may be bound in a reversible manner. The ability of the wall to bind and concentrate cations such as Ca^{2+} and Fe^{3+} at the membrane/wall interface [14,15] has been shown to be important for membrane function and the efficient secretion and folding of certain *Bacillus* secretory proteins [3,4,16,17].

Secretory proteins destined for the culture medium must traverse the wall as the last stage in the export process, and the physico-chemical properties of the wall dictate which interactions between secretory proteins and the wall are likely to occur. Thus the nature of these interactions is likely to be affected by the physico-chemical properties of both the secretory proteins and the wall. It has been suggested that the cell wall of *B. subtilis* acts as a 'barrier' to the secretion of certain heterologous proteins, such as human serum albumin (HSA), which is only released into

Abbreviations used: AmyL, *Bacillus licheniformis* α-amylase; AmyLQS, chimaeric α-amylase; AmyQ, *Bacillus amyloliquefaciens* α-amylase; AmyS, *Bacillus stearothermophilus* α-amylase; CWBP, cell-wall-binding protein; FDPB, finite difference Poisson–Boltzmann; GRASS, graphical representation and analysis of structure server; HSA, human serum albumin; IEF, isoelectric focusing; $t_{\frac{1}{2}}$, half-life.

[1] Present address: Department of Molecular and Experimental Medicine, The Scripps Research Institute, 10550 N. Torrey Pines Road, La Jolla, CA 92037, U.S.A.

[2] Present address: Carlsberg Research Center, Gamle Carlsbergvej 10, DK-2500 Valby, Denmark.

[3] To whom correspondence should be addressed (e-mail colin.harwood@ncl.ac.uk).

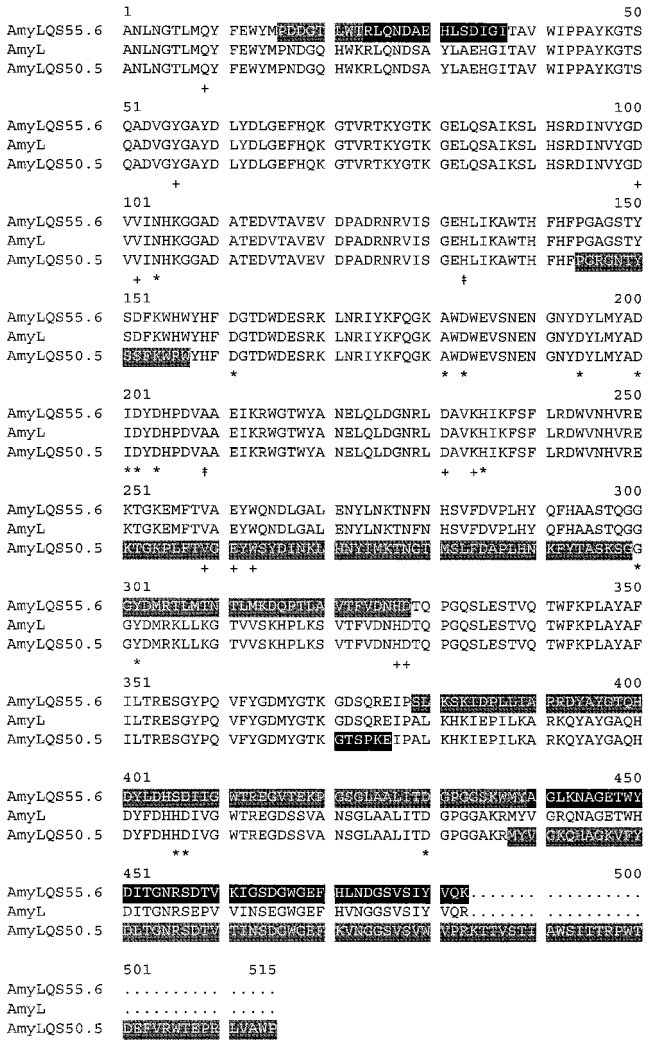

Figure 1 Protein-sequence alignment of wild-type AmyL and the chimaeric charge variants AmyLQS50.5 (high pI) and AmyLQS55.6 (low pI)

Regions of the chimaeric α-amylases originating from AmyS (grey) and AmyQ (black) are highlighted and amino acid residues implicated in Ca^{2+} binding (*), catalytic activity (+) or thermostability (‡) of AmyL are indicated under the sequences.

the culture medium at detectable levels following the removal of the wall [18].

Proteins which function within the wall, such as the autolysin LytC and the serine protease CWBP52, have pI values of 10.6 and 9.9 respectively [19,20], which ensure that these proteins remain firmly attached to the wall by electrostatic interactions. In contrast, we have shown previously that proteins that are naturally secreted into the culture medium by *B. subtilis* strain W23 are neutral in terms of charge (pI values in the range 6.5–7.0; see [21]), and this has generally been confirmed by analysis of putative secretory proteins identified within the genome sequence of *B. subtilis* 168 [22]. This may represent an important evolutionary adaptation to prevent proteins which are destined to exert their function in the extracellular environment from attaching inappropriately to the cell wall.

α-Amylases are ubiquitous Ca^{2+}-containing enzymes which hydrolyse α-D-(1 $\rightarrow$ 4) glycosidic linkages in starch and related carbohydrates. Ca^{2+} is required for the structural integrity of α-amylases such as AmyL [23–25]. Consistent with the structural topologies of other α-amylases and amylolytic enzymes, the structure of AmyL has three distinct domains [24]. The central N-terminal domain (domain A, residues 1–101 and 203–396) of AmyL is the most conserved domain throughout the α-amylases and is composed of a $(\beta/\alpha)_8$ barrel, with the active site and a conserved Ca^{2+}-binding site (Ca I) located on the C-terminal side of the barrel [24,25]. Domain B is a protrusion from domain A and is composed of a two long central β-strands (residues 111–121 and 133–140) wound around each other in a helical manner and four antiparallel β-strands. An α-helix found in the majority of α-amylases is replaced in AmyL by a stem–loop structure which provides the majority of the ligands for a novel linear metal-ion array, the Ca I–Na–Ca II triad [25]. The substrate-binding cleft is located in the interface between domains A and B, the structure of which is stabilized by the Ca I–Na–Ca II triad. The C-terminal domain of AmyL (domain C, residues 393–483) contains a Greek-key motif, and an additional Ca^{2+}-binding site (Ca III) is located at the interface of this domain with domain A and represents a second anchor point between these two domains [25].

To gain an insight into the potential influence of electrostatic interactions on late (that is, post-translocational) stages in the secretion pathway, we have constructed chimaeric variants of AmyL with modified net charge and have studied in detail their secretion from *B. subtilis* [5]. The chimaeric α-amylases (Figure 1) were designed, prior to the resolution of the crystal structure of AmyL [24], by replacing specific regions of the primary sequence of AmyL with corresponding regions of the related α-amylases from *Bacillus amyloliquefaciens* (AmyQ) and *Bacillus stearothermophilus* (AmyS) to increase or decrease the pI of the proteins in relation to wild-type AmyL (pI 7.0). The genes encoding the chimaeric α-amylases were then engineered using a PCR-based gene-splicing technique and expressed in *B. subtilis* [5].

In the present study we have used these charge variants of AmyL to investigate the hypothesis that engineered secretory proteins with an overall positive charge would interact strongly with the negatively charged cell wall, whereas proteins with an overall neutral or negative charge would interact weakly or might even be repelled by the cell wall. The present paper describes enzymic and physico-chemical properties of two chimaeric α-amylases, AmyLQS50.5 (pI 10.0) and AmyLQS55.6 (pI 5.0), which have, respectively, an increased net positive or negative charge as compared with AmyL (pI 7.0). These properties are discussed in relation to the potential influence of charge on late stages in the secretion of proteins from *B. subtilis*, and in particular the interaction of secretory proteins with the cell wall prior to release into the culture medium.

EXPERIMENTAL

Bacterial strains and growth

The bacterial strains and plasmids used in the present study are shown in Table 1. Strains were grown in 2 × YT medium [2 × YT = 1.6 % (w/v) tryptone/1 % (w/v) yeast extract/0.5 % NaCl], and chloramphenicol (6 μg/ml) was included in the growth media as required. For pulse–chase and immunoprecipitation, cultures were grown in Spizizen's minimal salts with 1 % ribose as a non-catabolite-repressing carbon source [26]. The α-amylases were expressed from genes integrated into the *xylR* gene on the chromosome, and their synthesis was inducible by the presence of 1 % (w/v) xylose in the culture medium, as described previously [4,6]. Cultures were grown at 37 °C with shaking (180 rev./min).

Table 1 Bacterial strains and plasmids

Strain/plasmid	Properties	Reference
Strain		
B. subtilis DN1885	α-Amylase (*amyE*) negative strain	[41]
Plasmids		
pCJ272	Integration vector, xylose-inducible *amyLQS55.6*, Cm^r	[5]
pKS408	Integration vector, xylose-inducible *amyL*, Cm^r	[5]
pKS405B	Integration vector, xylose-inducible *amyLQS50.5*, Cm^r	[5]

Quantification of α-amylase activity

The α-amylase activity of the purified proteins was measured using the Phadebas assay kit (Pharmacia Upjohn), as described by the manufacturer. One unit of α-amylase activity was defined as the amount of enzyme catalysing the hydrolysis of 1 μmol of glycosidic linkage/min at 37 °C.

Purification of α-amylases

α-Amylases were purified from spent culture media of *B. subtilis* grown at 37 °C for 5 days. AmyL and AmyLQS50.5 were purified using a preparative isoelectric focusing (IEF) cell (Rotofor; Bio-Rad). Proteins in culture supernatants were precipitated with 50 %-satd. $(NH_4)_2SO_4$, pelleted by centrifugation (10000 ***g***, 1 h, 4 °C] and resuspended in 9 ml of 5 mM sodium phosphate buffer (1.4 mM NaH_2PO_4/3.6 mM Na_2HPO_4, pH 7.2). Residual $(NH_4)_2SO_4$ was removed by dialysis against 1 litre of 5 mM sodium phosphate buffer for 48 h at 4 °C, with several changes of buffer. The dialysed solution was mixed with ampholytes [2 % (w/v), pH range 3–10; Bio-Rad] in sterile distilled water to a final volume of 55 ml. The Rotofor focusing cell was operated for 4–6 h as described by the manufacturer. Focused proteins were harvested as 20 fractions, and each fraction was assayed for α-amylase activity and analysed by SDS/PAGE. The fractions containing the majority of the α-amylase were dialysed for 72 h against 1 litre of 1 M NaCl to remove electrostatically bound ampholytes. The samples were then dialysed against 1 litre of 5 mM sodium phosphate buffer to remove the NaCl. Finally, the samples were concentrated by dialysis against 20 % (w/v) poly(ethylene glycol) 6000 in 5 mM sodium phosphate buffer for 1–2 h.

It was not possible to purify AmyLQS55.6 to homogeneity using preparative IEF owing to the presence of numerous contaminating proteins with pI values similar to that of this α-amylase. Consequently, AmyLQS55.6 was purified by adding $(NH_4)_2SO_4$ to the culture supernatant to a final concentration of 1 M and then applying the mixture to a Butyl Toyo Pearl column (25 ml) equilibrated with 1 M $(NH_4)_2SO_4$ in Tris/Ca buffer (10 mM Tris/HCl/2 mM $CaCl_2$, pH 7.0.). The column was washed, and the bound proteins were eluted with 2 mM $CaCl_2$ and then dialysed against 5 mM Tris/HCl/2 mM $CaCl_2$, pH 7.0. The dialysed proteins were then applied to a 50 ml Q-Sepharose anion-exchange column equilibrated with 10 mM Tris/Ca buffer, and the bound proteins eluted using a linear gradient over 10 column vol. of 0–0.3 M NaCl in 10 mM Tris/Ca buffer. The fractions containing α-amylase activity were pooled and, following the addition of $(NH_4)_2SO_4$ to a final concentration of 1 M, the solution was applied once again on to a Butyl Toyo Pearl column (25 ml). Bound proteins were eluted in fractions using a linear gradient from 1 to 0 M $(NH_4)_2SO_4$ in 10 mM Tris/Ca buffer over 5 column vol. Fractions containing α-amylase activity were pooled and dialysed against 10 mM sodium acetate/2 mM $CaCl_2$, pH 6.5. The dialysed protein solution was then applied to a 5 ml S-Sepharose column that was equilibrated with 10 mM sodium acetate/2 mM $CaCl_2$ at pH 4.5. Bound proteins were eluted using a linear gradient of 0–0.3 M NaCl in 10 mM sodium acetate buffer.

In all cases the purity of the α-amylases preparations was confirmed by SDS/PAGE using 10 % (w/v) acrylamide gels [27] with Coomassie Blue staining.

CD spectroscopy and homology modelling of α-amylases

Spectra of purified α-amylases were collected on a Jobin–Yvon CD6 spectrometer in the wavelength range 195–250 nm using a 0.1 mm cuvette at protein concentrations of 0.2–0.4 mg/ml.

The published co-ordinates of calcium-free AmyL (1BPL; see [24]) were used as the basis for homology modelling using the programme MODELER (Molecular Simulations Inc, San Diego; [28]). The more recent Ca^{2+}-containing structure of AmyL (1BLI; see [25]) was not used, because the finite difference Poisson–Boltzmann (FDPB) electrostatic calculations used currently do not include heteroatoms. The sequence alignment of the α-amylases (Figure 1) is largely unequivocal and residues corresponding to 182–192 of AmyL (which are not resolved in 1BPL) were deleted. For each protein, four models were calculated. As expected from the high sequence similarity and lack of gaps in the sequence alignment, the four structures were superimposable and one was chosen at random as the representative model structure.

The distribution of electrostatic potential was calculated using the Graphical Representation and Analysis of Structure Server (GRASS) at the University of Columbia [29]. The PARSE (**par**ameterization by **s**olvation **e**nergy) charge set was used in conjunction with the FDPB solver, and for this all hydrogen atoms were added to the PDB (protein database) file using the molecular-editor function of Quanta (Molecular Simulations). Results were stored as VRML (mark-up language) files and displayed on Netscape Navigator 4.07 with a Cosmo Software plug-in.

Determination of the temperature optima, pH optima and thermostability of the α-amylases

Purified protein solutions were diluted to a concentration of 0.15 μg/ml in 0.09 mM $CaCl_2$ and 1 ml samples were assayed for α-amylase activity using the Phadebas kit under the various test conditions. Temperature optima were determined by measuring α-amylase activity for 15 min at different temperatures. pH optima were determined by measuring α-amylase activities at 37 °C in the Britton–Robinson buffer system [30] at pH values between 4.0 and 11.0.

Thermostability was determined by incubating purified proteins (0.15 μg/ml) in 50 mM sodium acetate (pH 6.5)/10 mM $CaCl_2$ at 90 °C. Samples were removed at time intervals, and the degree of irreversible thermal inactivation of the α-amylases was then determined by measuring the residual α-amylase activity at 37 °C.

Protein concentration was determined spectrometrically at 280 nm using Beer's law and the following absorption coefficients (A_{280} [1]), calculated using the Composition function of the Lasergene software (DNASTAR Inc., Madison, WI, U.S.A.): 0.41 mg/ml for AmyL, 0.3 mg/ml for AmyLQS50.5 and 0.39 mg/ml for AmyLQS55.6.

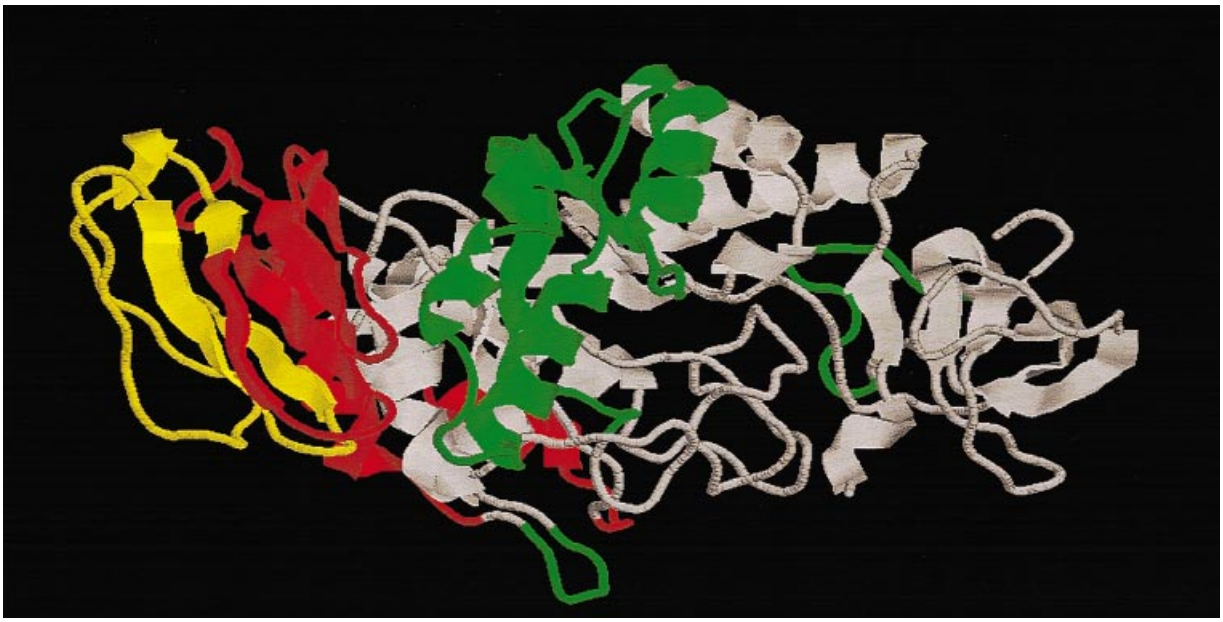

Figure 2 Ribbon representation drawn using RasMol [42] of the AmyL structure 1BPL [24] showing regions altered to create high- (AmyLQS50.5) and low-pI (AmyLQS55.6) variants

Red, regions changed in AmyLQS55.6; green, regions changed in AmyLQS50.5; yellow, regions changed in both.

Determination of pI

Proteins were precipitated from spent culture media with 50 %-satd. $(NH_4)_2SO_4$], resuspended in 5 mM sodium phosphate buffer and dialysed against the same buffer to remove residual $(NH_4)_2SO_4$. Protein solutions were then subjected to IEF with the Rotofor cell and the resultant fractions harvested and assayed for the presence of the various α-amylases using the Phadebas kit. The pH of the fraction containing the peak of α-amylase activity represented the pI of that particular enzyme.

Pulse–chase and immunoprecipitation

Exponentially growing cultures of *B. subtilis* were pulse-labelled with L-[^{35}S]methionine as described previously [6] and samples removed at the following time intervals; 0, 1, 3, 6, 10 and 20 min. Labelled α-amylases in whole culture samples and released into the growth medium [obtained by filtration through 0.45 μm PVDF filters (Whatman Limited, Maidstone, Kent, U.K.)] were immunoprecipitated and subjected to SDS/PAGE and fluorography. The relative amounts of precursor and mature α-amylases present at each time interval were determined by PhosphorImaging (PhosphorImager; Molecular Dynamics) using the associated software (ImageQuant version 3.22; Molecular Dynamics).

In vitro cell-wall-binding assay

The cell walls were isolated from *B. subtilis* 168 grown in phosphate-replete conditions as described previously [31] and had teichoic and teichuronic acid compositions of 0.927 and 0.145 μmol/mg of wall respectively. D-Alanyl esters of teichoic acids, which have the effect of neutralizing adjacent phosphate groups [14,32], were removed by washing wall samples (26 mg) several times in 500 μl aliquots of Tris/HCl at pH 8.0. Non-covalently bound molecules or ions were removed from the wall preparation by reducing the concentration of Tris/HCl from 1 M to 100 μM in 10-fold steps with subsequent washes. The wall material was then washed three times with 500 μl of distilled water and resuspended in 200 μl of distilled water.

The assay was carried out using purified AmyL, AmyLQS50.5, AmyLQS55.6 and HSA (Sigma) diluted to 25 ng/μl in 5 mM sodium phosphate buffer, pH 7.2. Protein samples (50 μl) and wall suspensions (35 μl) were mixed and incubated at 37 °C for 15 min to allow binding. Following binding, the walls were pelleted by microcentrifugation (11000 ***g***, room temperature, 5 min), the supernatants were transferred to new tubes and an equal volume of 2 × SDS/PAGE sample buffer was added to each supernatant sample followed by boiling for 5 min. The wall pellets were washed three times with 200 μl aliquots of distilled water and resuspended in sample buffer to give the same final volume as the supernatant samples. Bound proteins were released by boiling for 5 min.

The samples were subjected to SDS/PAGE [10 % (w/v) gels] followed by Western blotting [33] on to cellulose nitrate membranes (0.4 μm pore diameter; Anderman, Kingston-upon-Thames, Surrey, U.K.). Bands corresponding to the α-amylases or HSA were detected using polyclonal rabbit antisera raised against AmyL (provided by Novo Nordisk) or HSA (Sigma) respectively, and anti-rabbit IgG–horseradish peroxidase conjugate (Dako Immunochemicals A/S). The relative amounts of proteins were quantified using a Gel Documentation system (Gel-Doc II; Bio-Rad) and associated Molecular Analyst software.

RESULTS

CD spectroscopy and homology modelling of α-amylases

As expected from the known X-ray crystallographic structure of AmyL (Figure 2), the CD spectra of AmyL, AmyLQS50.5 and

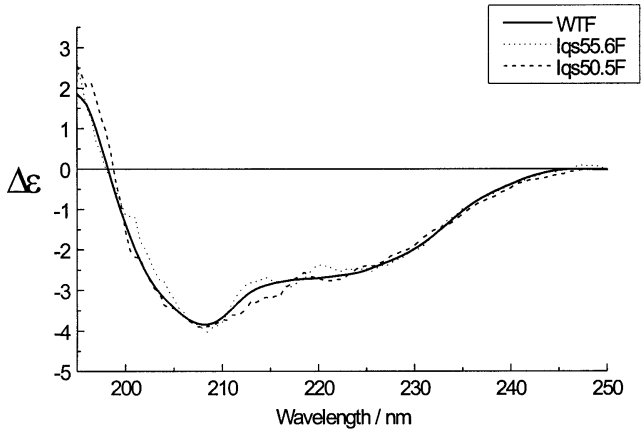

Figure 3 Far-UV CD of wild-type AmyL ('WTF'), AmyLQS50.5 ('Iqs50.5F') and AmyLQS55.6 ('Iqs55.6F')

Samples in 50 mM sodium phosphate, pH 7.0, were measured in a 0.1-mm-path-length cuvette at 25 °C. Protein concentrations were 0.4 mg/ml (AmyL), 0.17 mg/ml (AmyLQS50.5) and 0.2 mg/ml (AmyLQS55.6). Dichroism is expressed as mean-residue absorption-coefficient difference ($\Delta\epsilon$) [43].

AmyLQS55.6 showed mixed α/β structures (Figure 3) [24,25]. No differences of any significance were observed between the CD spectra of AmyL and the chimaeric α-amylases (Figure 3), indicating that both chimaeric enzymes retained the native fold and that homology modelling of the chimaeric proteins was feasible.

Homology modelling with the subsequent calculation of electrostatic potential allowed the predicted surface charge distribution of the α-amylases to be investigated (Figure 4). Wild-type AmyL (Figure 4A) showed a relatively even distribution of positive and negative charge on the surface, with a high concentration of negative charge within the substrate-binding cleft. In contrast, the chimaeric α-amylases show clear differences in the distribution of surface electrostatic charge and, as expected, AmyLQS50.5 (Figure 4B) and AmyLQS55.6 (Figure 4C) showed increased positive and negative surface charge respectively. Of special interest was the conservation of negative charge within the substrate-binding cleft of the high-pI variant AmyLQS50.5, despite a visible increase in positive charge elsewhere on the surface (Figure 4B).

Characterization of the chimaeric α-amylases

The pI values of the α-amylases precipitated from culture media were determined by IEF using the Rotofor. AmyLQS55.6, AmyL and AmyLQS50.5 were found to have pI values of 5.0, 7.0 and 10.0 respectively (Figure 5), confirming that the changes engineered into AmyL had the desired affects on net charge. These data were in agreement with the electrostatic-surface-charge predictions (Figure 4). The reason for the broader pI profile of AmyL was not investigated, but could in part be accounted for by deamidation, to which this enzyme is susceptible at low pH values (A. Svendsen and S. T. Jørgensen, unpublished work).

The specific activities (Table 2) of the purified α-amylases were determined in 100 mM sodium phosphate buffer, pH 6.1. The specific activity of the high-pI variant AmyLQS50.5 was $\approx 70\%$ of that of AmyL, a decrease that can almost completely be accounted for by the change in the pH optimum of this enzyme (see below and Figure 6C). In contrast, the specific activity of the

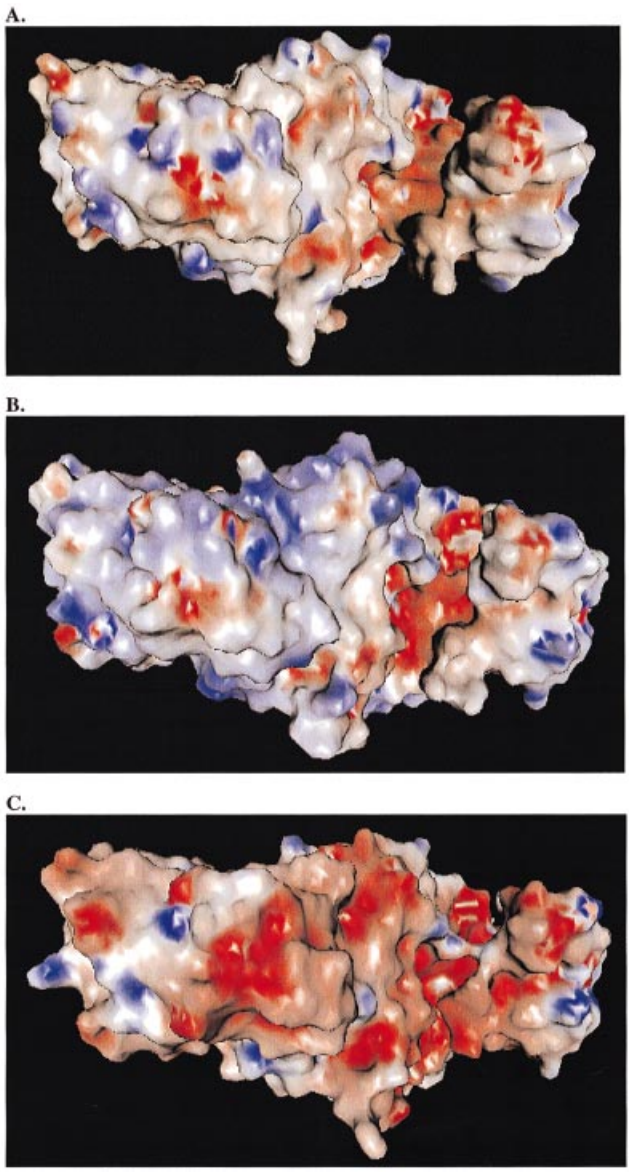

Figure 4 Distribution of surface charge on AmyL (A) and chimaeric variants AmyLQS50.5 (pI 10.0) (B) and AmyLQS55.6 (pI 5.0) (C)

The Figures represent the molecules in the same orientation as in Figure 2, with the active-site cleft to the right. Surface charge distributions were calculated using the GRASS software as described in the text; negative charge is shown in red and positive charge is shown in blue. The conservation of negative charge in the active-site cleft explains why the enzymic activity is conserved in AmyLQS50.5, despite its high overall pI.

low-pI variant, AmyLQS55.6, was significantly higher ($\approx 62\%$ increase) than that of AmyL.

Two important features of AmyL which make this enzyme of commercial importance are its high temperature optimum (75–95 °C; see [34,35]) and enhanced thermostability compared with the related α-amylases AmyQ and AmyS [35–37]. We therefore determined the temperature optima and thermostabilities of the purified α-amylases.

When expressed as a function of temperature, the activity profiles of the chimaeric α-amylases were almost identical with that of AmyL, with the maximum enzyme activities at ≈ 75 °C (Figure 6A). The thermostability of α-amylases was investigated

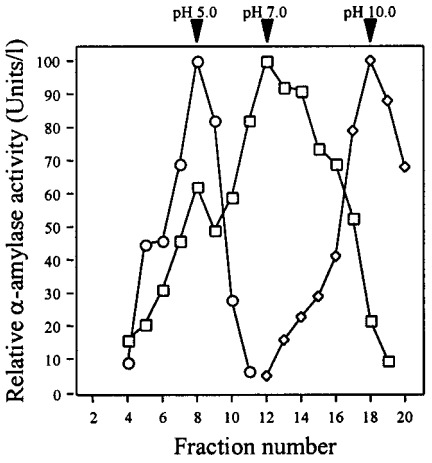

Figure 5 Isoelectric focusing of α-amylases precipitated with $(NH_4)_2SO_4$ from spent culture media using the Rotofor cell

□, AmyL; ◇, AmyLQS50.5; ○, AmyLQS55.6.

Table 2 Number of charged amino acids, pI values and enzyme specific activities of AmyL and chimaeric α-amylases

The positively charged amino acids are lysine, arginine and histidine; the negatively charged amino acids are aspartic acid and glutamic acid.

	Number of charged amino acids			
α-Amylase	Positive	Negative	pI of mature protein	Specific activity (units/mg of protein)
AmyL	73	62	7.0	6530
AmyLQS50.5	82	60	10.0	4570
AmyLQS55.6	64	67	5.0	10500

by measuring the α-amylase activity remaining after incubation of purified proteins at 90 °C. Following a slight initial increase, the enzyme activity of all the α-amylases decreased with time (Figure 6B). AmyL shows enhanced thermostability compared with other α-amylases, with an estimated half-life ($t_{\frac{1}{2}}$) of irreversible thermal inactivation of 84 min. The chimaeric α-amylases were more susceptible to irreversible thermal inactivation than AmyL, with estimated $t_{\frac{1}{2}}$ values of 32 and 20 min for AmyLQS55.6 and AmyLQS50.5 respectively.

A comparison of the pH profiles of the chimaeric α-amylases with that of AmyL (Figure 6C) revealed significant, but relatively small, differences between the enzymes (Figure 6C). The most notable difference was that AmyL exhibited optimal activity over a broad range of pH values ($\approx$ 6.5 to 8.0), while the chimaeric proteins exhibited optimal activities over narrow pH ranges. AmyLQS50.5 had a pH optimum of $\approx$ 7.5, while that of AmyLQS55.6 was $\approx$ 6.5.

Influence of charge on cell-wall-binding activity

For efficient release into the culture medium, secretory proteins must traverse the cell-wall cylinder rapidly, avoiding interactions with components of the wall. We have developed an *in vitro* assay to assess the capacity of proteins in their native (that is, fully folded) conformations to bind to extracted *B. subtilis* cell walls. The assay was used to determine the wall-binding characteristics of wild-type AmyL and the charge-modified chimaeras. In addition, the wall binding of HSA (pI 5.2; see [38]), an eukaryotic protein whose secretion from *B. subtilis* has been suggested to be blocked by interaction with the cell wall [18], was also tested.

When the binding of AmyL (pI 7.0) to extracted wall was tested, about a quarter of the added protein was recovered from the wall fraction, whereas the remainder was present in the supernatant (Table 3). Consistent with our hypothesis, AmyLQS50.5 (pI 10.0) was recovered exclusively from the wall fraction, whereas AmyLQS55.6 (pI 5.0) was recovered exclusively from the supernatant (Table 3). Similar amounts of HSA were bound to the extracted cell wall as was observed for AmyL.

These data demonstrate that, under the assay conditions used, the net charge of AmyL and its engineered chimaeras influenced the extent to which they interacted with the cell wall *in vitro*; the chimaera with an overall positive charge showed considerable wall binding, whereas the negatively charged chimaera showed no interaction with the wall.

Coupled pulse–chase and immunoprecipitation techniques

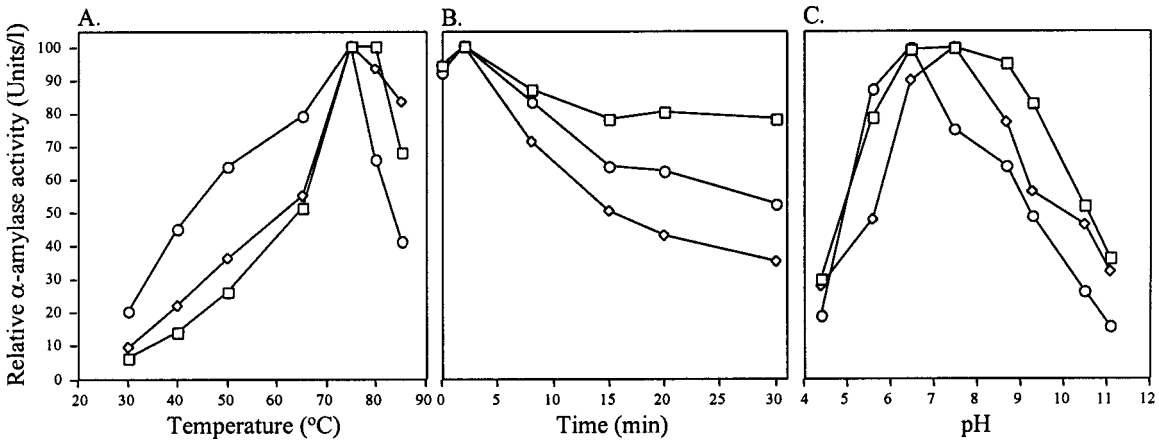

Figure 6 Relative activities of AmyL (□), AmyLQS50.5 (◇) and AmyLQS55.6 (○)

(**A**) Temperature–activity profiles of the α-amylases determined in 0.09 mM $CaCl_2$. (**B**) Residual α-amylase activity (at 37 °C) following incubation at 90 °C in 50 mM sodium acetate (pH 6.5)/10 mM $CaCl_2$. (**C**) pH–activity profiles of the α-amylases determined in Britton–Robinson buffer.

Table 3 *In vitro* binding of AmyL, chimaeric derivative and HSA to cell walls isolated from *B. subtilis*

Binding was carried out using duplicate protein samples at 37 °C in 5 mM sodium phosphate, pH 7.2, and quantified by quantitative Western blotting.

	Total protein recovered (%)	
α-Amylase	In the supernatant	With the wall fraction
AmyL	74	26
AmyLQS50.5	0	100
AmyLQS55.6	100	0
HSA	76	24

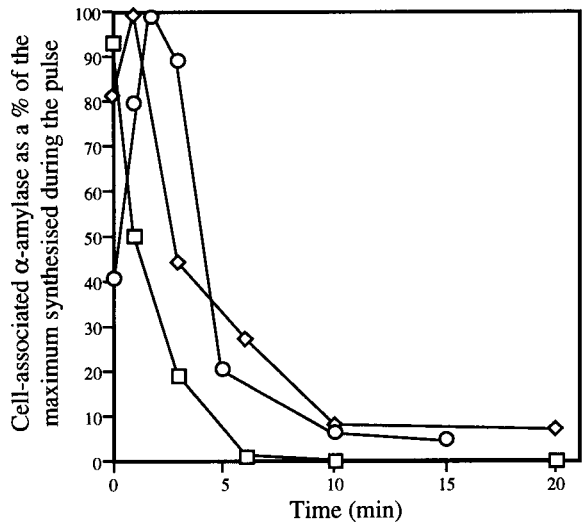

Figure 7 Post-translocational binding of α-amylases to the cell wall during secretion from *B. subtilis*

Cell-associated mature forms of AmyL (□), AmyLQS55.6 (○) and AmyLQS50.5 (◇) were measured by subtracting PhosphorImaging data for released α-amylase from those obtained for the whole culture samples, as described previously [6]. The amount of α-amylase at each time interval is expressed as a percentage of the maximum amount of α-amylase (precursor plus mature) synthesized during the pulse.

were used to investigate post-translocational association of the mature forms of wild-type AmyL and the chimaeric proteins during secretion from *B. subtilis* DN1885. PhosphorImaging data from pulse–chase experiments on *B. subtilis* DN1885 *xylR*::pKS408, DN1885 *xylR*::pCJ272 and DN1885 *xylR*::pKS405B were used to determine the proportion of mature AmyL, AmyLQS55.6 and AmyLQS50.5 respectively remaining cell-associated with time post-chase as described previously [6].

The amounts of cell-associated mature forms of the α-amylases decreased with time as a consequence of a combination of cell-associated degradation and release into the growth medium (Figure 7). Cell-associated AmyL decreased rapidly with time, and by ≈ 7 min post-chase, none of the AmyL synthesized during the pulse remained cell-associated. In contrast, at all times post-chase, more mature AmyLQS55.6 and AmyLQS50.5 was cell-associated; at 10 min post-chase, 5–9 % of the maximum synthesized during the pulse remained cell-associated (Figure 7). This is likely to represent a considerable degree of wall association, since both of the chimaeric amylases undergo more extensive cell-associated degradation than AmyL ([4]; C. L. Jensen, K. Stephenson, S. T. Jørgensen and C. R. Harwood, unpublished work). In the case of AmyLQS50.5, this may reflect binding between the positively charged protein and the negatively charged cell wall. In the case of AmyLQS55.6, this may reflect either charge repulsion between the folded protein and the cell wall or binding between the wall and mis-folded protein.

These *in vivo* data suggest that, as a consequence of electrostatic interactions with components of the cell wall, a greater proportion of AmyLQS50.5 binds to the wall following translocation across the cytoplasmic membrane, as compared with AmyL, which is neutral in terms of net charge. This is in agreement with the data obtained from the *in vitro* wall-binding studies described above.

DISCUSSION

The chimaeric α-amylases were designed and engineered to facilitate studies on the significance of net charge for the interaction of proteins with the *B. subtilis* cell wall, an area which had not previously been studied in detail. The similarity of the CD spectra of purified chimaeric α-amylases to wild-type AmyL justified the use of a homology-modelling approach to investigate the surface charge of the α-amylases. The high level of sequence identity (Figure 1) ensures that the MODELER software fitted the unknown sequences to the AmyL structure with little or no ambiguity. Hence, the positions of the charged residues used for the Delphi calculations [39] are likely to be realistic. The FDPB method for electrostatic-charge distribution proved to be much more revealing than a simple inspection of the distribution of charged amino acids, since it accounted for charge–charge interactions and the effects of the low dielectric constant of the protein. The protein surface electrostatic modelling revealed why the chimaeric proteins were still functional α-amylases by highlighting the conservation of charge near the substrate-binding groove and active site, and indicated regions elsewhere on the protein molecules where the charge affects were greatest.

Although the engineered proteins showed the alterations in pI predicted from protein-sequence data and charge modelling, other major characteristics, such as temperature and pH of maximum activity, were largely unaffected. α-Amylases interact with the substrate at the substrate-binding cleft and via multiple binding sites on the enzyme surface [25]. The increased specific activity of AmyLQS55.6 may be at least partly explained using the surface-charge model, which shows the extension of the negative charge from the substrate-binding cleft on to the surface of the molecule; the converse may also hold true for positively charged AmyLQS50.5.

Thermostability is a feature relevant to the industrial importance of AmyL [35] and related α-amylases. Whereas AmyL was relatively resistant to irreversible thermal inactivation ($t_{\frac{1}{2}} \approx$ 84 min), AmyLQS50.5 ($t_{\frac{1}{2}} \approx$ 20 min) and AmyLQS55.6 ($t_{\frac{1}{2}} \approx$ 32 min) were both less thermostable. With the exception of Ser^{406} of AmyLQS55.6, which corresponds to His^{406} of AmyL involved in Ca^{2+} binding, all of the other amino acid residues implicated in Ca^{2+} binding [25], catalytic activity [24] or thermostability [40] of AmyL are conserved in AmyLQS50.5 and AmyLQS55.6 (Figure 6). Therefore it is difficult to predict the nature of the differences in specific activity and thermostability of the chimaeric α-amylases reported in the present paper.

The yields of the chimaeric enzymes in the culture medium were found to be greatly reduced in comparison with AmyL [5], and we have shown that this was due neither to differences in the transcriptional activity of the genes encoding the chimaeric enzymes [5] nor to large reductions in their specific activities (the present study). Instead we have shown they were due to increased

post-translocational, but cell-associated, proteolysis [5]. For AmyLQS50.5 at least, this appears to be due to a combination of its reduced rate of folding on the *trans* side of the membrane [4] and the susceptibility of incompletely folded forms to extracellular, but cell-associated, proteases. The decreased rate of folding presumably increases the access time for cell-associated proteases such as CWBP52 to target sites that are not accessible in the native structure. It is likely that the same applies to AmyLQS55.6.

In the *in vitro* wall-binding assay, AmyLQS50.5 has an higher affinity for isolated cell walls than either native AmyL or AmyLQS55.6. In addition, we have shown previously that the cell wall has the capacity to retard the transition of AmyLQS50.5 from the unfolded to the fully folded (enzymically active) conformation, whereas the folding of AmyL was unaffected by the presence of wall [4]. As a consequence of the more extensive cell-associated degradation that the chimaeric α-amylases undergo co-/post-translocationally, it is more difficult to demonstrate the effects of wall binding *in vivo*. However, in pulse–chase experiments, all of the processed AmyL that survives cell-associated degradation is recovered from the culture supernatant (results not shown), whereas, in the case of AmyLQS50.5, a proportion of the protein which is not degraded remains in the cell-associated fraction.

HSA (pI 5.2) exhibited *in vitro* wall-binding characteristics that were comparable with those of AmyL, suggesting that, on the basis of electrostatic interactions at least, the wall is unlikely to represent a significant barrier to the secretion of HSA [18]. Instead, cell-associated degradation could account for the failure to detect significant amounts of this protein in the culture medium [18], as was the case for some of the chimaeras of AmyL [5].

Prior to these studies there was little information on the potential influence of the cell wall on the secretion of proteins from *B. subtilis*. We have developed an approach that allows us to investigate the importance of the cell wall in the secretion process by engineering a normally well-secreted *Bacillus* α-amylase, AmyL, in such a way as to modulate its interactions with the *B. subtilis* wall. The data demonstrates that the wall cylinder has the potential to retard the passage of positively charged secretory proteins to a greater extent than neutral or negatively charged proteins. *In vivo*, the binding of secretory proteins to the cell wall, either during or following folding into the native conformation, has the effect of localizing the protein in close proximity to cell-associated extracellular proteases such as CWBP52 [20]. However, any wall-bound protein not degraded would be expected to be eventually released into the growth medium as a consequence of the wall turnover which accompanies growth [31].

Finally, these studies point to additional factors that may need to be considered when using *Bacillus* species as hosts for high-level secretion of engineered native or heterologous proteins. In these studies we have examined the effect on secretion of the overall positive charge of a protein. The data showing interactions between the wall and AmyLQS50.5 indicate that there may be value in tailoring the charge of the cell wall so as to avoid or reduce the likelihood of interactions between the wall and secretory proteins that may detrimentally affect the secretion of the latter.

This work was supported by grants from the EC Biotech programme (contract numbers BIO2-CT93-0254 and BIO4-CT96-0097), the U.K. Biotechnology and Biological Sciences Research Council (BBSRC) and Novo Nordisk A/S. We are grateful to B. R. Nielsen of Novo Nordisk A/S for the purification of the AmyLQS55.6. The work was carried out within the framework of the European *Bacillus* Secretion Group (EBSG).

REFERENCES

1 Ferrari, E., Jarnagin, A. S. and Schmidt, B. F. (1993) Commercial production of extracellular enzymes. In *Bacillus subtilis* and other Gram-positive Bacteria: Biochemistry, Physiology and Molecular Genetics (Sonenshein, A. L., Hoch, J. A. and Losick, R., eds.), pp. 917–937, American Society for Microbiology, Washington DC
2 Simonen, M. and Palva, I. (1993) Protein secretion in *Bacillus* species. Microbiol. Rev. **57**, 109–137
3 Chambert, R., Haddaoui, E. A. and Petit-Glatron, M.-F. (1995) *Bacillus subtilis* levansucrase: the efficiency of the second stage of secretion is modulated by external factors assisting folding. Microbiology **141**, 997–1005
4 Stephenson, K., Carter, N. M., Harwood, C. R., Petit-Glatron, M.-F. and Chambert, R. (1998) The influence of protein folding on the secretion of α-amylases from *Bacillus subtilis*. FEBS Lett. **430**, 385–389
5 Jensen, C. L., Stephenson, K., Jørgensen, S. T. and Harwood, C. R. (2000) Cell-associated degradation affects yield of secreted engineered and heterologous proteins in the *Bacillus subtilis* expression system. Microbiology, in the press
6 Stephenson, K. and Harwood, C. R. (1998) The influence of a cell-wall-associated protease on the production of α-amylase by *Bacillus subtilis*. Appl. Environ. Microbiol. **64**, 2875–2881
7 Ito, K. and Beckwith, J. (1981) Protein localization in *E. coli*: is there a common step in the secretion of periplasmic and outer-membrane proteins? Cell **24**, 707–717
8 Lee, C., Li, P., Inouye, H., Brickman, E. R. and Beckwith, J. (1989) Genetic studies on the inability of β-galactosidase to be translocated across the *Escherichia coli* cytoplasmic membrane. J. Bacteriol. **171**, 4609–4616
9 Rogers, H. J., Perkins, H. R. and Ward, J. B. (1980) Microbial Cell Walls and Membranes, Chapman and Hall, London.
10 Ward, J. B. (1981) Teichoic and teichuronic acids: Biosynthesis, assembly and location. Microbiol. Rev. **45**, 211–243
11 Archibald, A. R., Hancock, I. C. and Harwood, C. R. (1993) Cell wall structure, synthesis and turnover. In *Bacillus subtilis* and other Gram-positive Bacteria: Biochemistry, Physiology and Molecular Genetics (Sonenshein, A. L., Hoch, J. A. and Losick, R., eds.), pp. 381–410, American Society for Microbiology, Washington, DC
12 Beveridge, T. J. and Murray, R. G. E. (1976) Uptake and retention of metals by cell walls of *Bacillus subtilis*. J. Bacteriol. **127**, 1502–1518
13 Beveridge, T. J. and Murray, R. G. E. (1980) Sites of metal deposition in the cell wall of *Bacillus subtilis*. J. Bacteriol. **141**, 1876–1887
14 Hepstinall, S., Archibald, A. R. and Baddiley, J. (1970) Teichoic acids and membrane function in bacteria. Nature (London) **225**, 519–521
15 Hughes, A. H., Hancock, I. C. and Baddiley, J. (1973) The function of teichoic acids in cation control in bacterial membranes. Biochem. J. **132**, 83–93
16 Petit-Glatron, M.-F., Grajcar, L., Munz, A. and Chambert, R. (1993) The contribution of the cell wall to a transmembrane calcium gradient could play a key role in *Bacillus subtilis* protein secretion. Mol. Microbiol. **9**, 1097–1106
17 Leloup, L., Haddaoui, E. A., Chambert, R. and Petit-Glatron, M.-F. (1997) Characterisation of the rate-limiting step of the secretion of *Bacillus subtilis* α-amylase overproduced during the exponential phase of growth. Microbiology **143**, 3295–3303
18 Saunders, C. W., Schmidt, B. J., Mallonee, R. L. and Guyer, M. S. (1987) Secretion of human serum albumin from *Bacillus subtilis*. J. Bacteriol. **169**, 2917–2925
19 Lazarevic, V., Margot, P., Soldo, B. and Karamata, D. (1992) Sequencing and analysis of the *Bacillus subtilis lytRABC* divergon: a regulatory unit encompassing the structural genes of the *N*-acetylmuramoyl-L-alanine amidase and its modifier. J. Gen. Microbiol. **138**, 1949–1961
20 Margot, P. and Karamata, D. (1996) The *wprA* gene of *Bacillus subtilis* 168, expressed during exponential growth, encodes a cell-wall-associated protease. Microbiology **142**, 3437–3444
21 Coxon, R. D. (1990) Factors affecting protein export from *Bacillus subtilis*. Ph.D. Thesis, University of Newcastle upon Tyne
22 Kunst, F., Ogasawra, N., Moszer, I., Albertini, A. M., Alloni, G., Azevedo, V., Bertero, M. G., Bessieres, P., Bolotin, A., Borchert, S. et al. (1997) The complete genome sequence of the Gram-positive bacterium *Bacillus subtilis*. Nature (London) **390**, 249–256
23 Violet, M. and Meunier, J.-C. (1989) Kinetic studies of the irreversible thermal inactivation of *Bacillus licheniformis* α-amylase. Biochem. J. **263**, 665–670
24 Machius, M., Weigand, G. and Huber, R. (1995) Crystal structure of calcium-depleted *Bacillus licheniformis* α-amylase at 2.2Å resolution. J. Mol. Biol. **246**, 545–559
25 Machius, M., Declerck, N., Huber, R. and Wiegand, G. (1998) Activation of *Bacillus licheniformis* alpha-amylase through a disorder → order transition of the substrate-binding site mediated by a calcium-sodium-calcium metal triad. Structure **6**, 281–292
26 Spizizen, J. (1958) Transformation of biochemically deficient strains of *Bacillus subtilis* by deoxyribonucleate. Proc. Natl. Acad. Sci. U.S.A. **44**, 1072–1078
27 Laemmli, U.K. (1970) Cleavage of structural protein during the assembly of the head of bacteriophage T4. Nature (London) **227**, 680–685

28 Sali, A. and Blundell, T. L. (1993) Comparative protein modelling by satisfaction of spatial restraints. J. Mol. Biol. **234**, 779–815
29 Nayal, M., Hitz, B. C. and Honig, B. (1999) GRASS: a server for the graphical representation and analysis of structures. Protein Sci. **8**, 676–679
30 Britton, H. T. S. and Robinson, A. R. (1931) The use of the antimony-antimonous oxide electrode in the determination of the concentration of hydrogen ions and in potentiometric titrations. J. Chem. Soc. **5**, 458–473
31 Merad, T., Archibald, A. R., Hancock, I. C., Harwood, C. R. and Hobot, J. A. (1989) Cell wall assembly in *Bacillus subtilis*: visualization of the old and new material by electron microscopic examination of samples stained selectively for teichoic acid and teichuronic acid. J. Gen. Microbiol. **135**, 645–655
32 Ellwood, D. C. and Tempest, D. W. (1972) Effects of environment on bacterial wall content and composition. Adv. Microbial Physiol. **7**, 83–117
33 Towbin, H., Staehelin, T. and Gordon, J. (1979) Electrophoretic transfer of proteins from SDS and acid/urea polyacrylamide gels to nitrocellulose sheets: procedure and some applications. Proc. Natl. Acad. Sci. U.S.A. **76**, 4350–4354
34 Ortlepp, S. A., Ollington, J. F. and McConnell, D. J. (1983) Molecular cloning in *Bacillus subtilis* of a *Bacillus licheniformis* gene encoding a thermostable α-amylase. Gene **23**, 267–276
35 Suzuki, Y., Ito, N., Yuuki, T., Yamagata, H. and Udaka, S. (1989) Amino acid residues stabilizing a *Bacillus* α-amylase against irreversible thermoinactivation. J. Biol. Chem. **264**, 18933–18938
36 Tomazic, S. J. and Klibanov, A. M. (1988) Mechanisms of irreversible thermal inactivation of *Bacillus* α-amylases. J. Biol. Chem. **263**, 3086–3091
37 Tomazic, S. J. and Klibanov, A. M. (1988) Why is one *Bacillus* α-amylase more resistant against irreversible thermoinactivation than another? J. Biol. Chem. **263**, 3092–3096
38 Denton, K. A. and Harris, R. (1995) High-performance capillary electrophoretic separation of human serum albumin using a neutral coated capillary. J. Chromatogr. **705**, 335–341
39 Gilson, M. K. and Honig, B. (1988) Calculation of the total electrostatic energy of a macromolecular system: solvation energies, binding energies and conformational analysis. Proteins **4**, 7–18
40 Declerck, N., Machius, M., Chambert, R., Wiegand, G., Huber, R. and Gaillerdin, C. (1997) Hyperthermostable mutants of *Bacillus licheniformis* α-amylase: thermodynamic studies and structural interpretation. Protein Eng. **10**, 541–549
41 Diderichsen, B., Wedsted, U., Hedegaard, L., Jensen, B. R. and Sjöholm, C. (1990) Cloning of *aldB*, which encodes α-acetolactate decarboxylase, an exoenzyme from *Bacillus brevis*. J. Bacteriol. **172**, 4315–4321
42 Sayle, R. A. and Milner-White, E. J. (1995) RASMOL: biomolecular graphics for all. Trends Biochem. Sci. **20**, 374–376
43 Fasman, G. D. (1996) Circular Dichroism and the Conformational Analysis of Biomolecules, Plenum Press, New York

Received 18 January 2000/25 April 2000; accepted 25 May 2000